Heat-induced coarsening of layer-by-layer assembled mixed Au and Pd nanoparticles

Young-Seok Shon[*1], Dayeon Judy Shon[1a], Van Truong[1b], Diego J. Gavia[1c],
Raul Torrico[2d] and Yohannes Abate[**2]

[1]*Department of Chemistry and Biochemistry, California State University Long Beach,
1250 Bellflower Blvd., Long Beach, CA 90840, USA*
[2]*Department of Physics and Astronomy, California State University Long Beach,
1250 Bellflower Blvd., Long Beach, CA 90840, USA*

Abstract. This article shows the coarsening behavior of nanoparticle multilayers during heat treatments which produce larger metallic nanostructures with varying shapes and sizes on glass slides. Nanoparticle multilayer films are initially constructed via the layer-by-layer self-assembly of small and monodispersed gold and/or palladium nanoparticles with different compositions (gold only, palladium only, or both gold and palladium) and assembly orders (compounding layers of gold layers over palladium layers or vice versa). Upon heating the slides at 600℃, the surface nanoparticles undergo coalescence becoming larger nanostructured metallic films. UV-Vis results show a clear reliance of the layering sequence on the optical properties of these metal films, which demonstrates an importance of the outmost (top) layers in each nanoparticle multilayer films. Topographic surface features show that the heat treatments of nanoparticle multilayer films result in the nucleation of nanoparticles and the formation of metallic cluster structures. The results confirm that different composition and layering sequence of nanoparticle multilayer films clearly affect the coalescence behavior of nanoparticles during heat treatments.

Keywords: coarsening; nanoparticles; gold; palladium; nanostructures; optical microscopy

1. Introduction

Despite being encapsulated by stabilizing ligands or surfactants, nanoscale metallic species obtained by bottom-up solution chemistry are often vulnerable to changes in size and shape when they are exposed to heat or light irradiation (Sugden *et al.* 2010, Hrbek *et al.* 2008). Although a tremendous amount of research has been concentrated in the area of metal nanoparticles, there is some deficiency in studies focusing on thermally induced changes in the particle morphology

∗Corresponding author, Professor, E-mail: ys.shon@csulb.edu
∗∗Corresponding author, Professor, E-mail: yabate@csulb.edu
[a]High School Volunteer Student, E-mail: dshon@caltech.edu
[b]Undergraduate Student, E-mail: mangosteen83@gmail.com
[c]M.S. Student, E-mail: djgavia@ymail.com
[d]M.S. Student, E-mail: rctorrico@gmail.com

when such species exist on a well-defined surface (Scarpettini and Bragas 2010, Sun *et al.* 2013).

Transparent nanostructured metal films are potentially important materials in medical diagnostics, photonics, molecular sensing, catalysis, and other technological applications (Stewart *et al.* 2008, Szunerlts *et al.* 2008, Zamborini *et al.* 2012). The increased application of such engineered nanomaterials has generated a need to define the impact of their dynamic behaviors on both their physical and chemical properties (Karakouz *et al.* 2009, Lee *et al.* 2012). For example, the nature and extent of transformations (e.g., aggregation, dissolution, and migration) must be understood before significant progress can be made toward predicting device performances.

Recently, we reported the preparation of nanostructured gold island films with different grain sizes using the self-assembly/heating of nanoparticle multilayer films of small (1-3 nm) gold nanoparticles (Shon *et al.* 2011, Vaccarello *et al.* 2012). Our preparation method for nanoisland films employed the layer-by-layer self-assembly method (Srivastava and Kotov 2008), which allows us to easily control the composition and structure of nanoparticle multilayer films. The scope of this current study is to understand how different multilayer construction protocols affect the overall structure of these metallic films. Specifically, this research investigates the transformation of Au and Pd bimetallic nanostructured films instigated by high temperature heating, which fuses assembled nanoparticles during the heat induced removal of organic binders and linkers on solid supports. In particular, understanding the effects on the optical and topographical properties of engineered nanoparticle films was the focal point of our research.

2. Experimental section

2.1 Materials

The following materials were purchased from the indicated suppliers and used as received: Hydrogen tetrachloroaurate ($HAuCl_4•3H_2O$), potassium tetrachloropalladate (K_2PdCl_4), glutathione (GSH, reduced form), 6-bromohexanoic acid, tetra-n-octylammonium bromide (TOAB), toluene, sodium borohydride ($NaBH_4$), and 3-mercaptopropyl trimethoxysilane (MPTS) were purchased from ACROS. Ethanol, glass microscope slides, hydrochloric acid, sulfuric acid, and 30% hydrogen peroxide were purchased from Fisher Scientific. Poly (allylamine hydrochloride) (PAH; MW *ca.* 70,000) was purchased from Sigma-Aldrich. Spectra/Por cellulose ester (CE) dialysis membranes (M.Wt.= 8,000-10,000 Daltons) were purchased from Spectrum Laboratories, Inc. Water was purified by Barnstead NANOpure Diamond ion exchange resins purification unit.

2.2 Synthesis of glutathione-functionalized gold nanoparticles (GS-AuNP)

To 50 mL of cooled (0℃) methanol, 98.5 mg (0.25 mmol) of $HAuCl_4·3H_2O$ was added and the reaction mixture was stirred until completely dissolved. To this yellow solution, 307.3 mg (1.0 mmol) of glutathione was added and the mixture was allowed to stir for an additional 30 min. Following this reaction period, a 0.2 M (94.6 mg, 12.5 mL) cooled aqueous solution of $NaBH_4$ was added to the mixture under vigorous stirring. The dark brown reaction mixture was let stirred for 1 h and the resulting precipitate was separated by centrifugation. To wash the crude precipitate, several 1 mL increments of methanol were added and then removed, followed by the addition and removal of 1 mL of ethanol. The washed product was allowed to dry in a vacuum oven over night.

A 36.0 mg of the dried crude product was dissolved in 14 mL of nanopure water and heated to 55°C with stirring. To the dark brown solution, 112 mg of GSH was added and the reaction was allowed to proceed for 90 min under heating and air bubbling directly in the mixture. After the reaction period, the brownish solution was separated from any unreacted crude product by centrifugation and purified by adding methanol to induce precipitation, which was then further washed with several increments of 1 mL methanol. The washed product was allowed to dry in a vacuum oven over night.

2.3 Synthesis of 6-mercaptohexanoic acid-functionalized Pd nanoparticles (MHA-PdNP)

An aqueous solution of 131 mg of K_2PdCl_4 (0.4 mmol) and a toluene solution (25 mL) containing 1.09 g of TOAB (2.0 mmol) were mixed and continuously stirred until the organic layer turned dark orange and the aqueous layer turned clear. Such color change indicated the completion of the phase transfer of $PdCl_4^{2-}$ from the aqueous phase to the organic phase. The organic layer was collected in a 250 mL round-bottom flask and the aqueous layer was discarded. A 200 mg (0.80 mmol, MW = 250.29 g/mol) of sodium ω-carboxylate-*S*-hexanethiosulfate (Lohse *et al.* 2010) dissolved in 10 mL of 25% methanol was added to the organic layer along with an additional 1.09 g of TOAB (2.0 mmol). Subsequently, the mixture was continuously stirred for 15 min. A 303 mg of $NaBH_4$ (8.0 mmol) in 7 mL of nanopure water was freshly prepared and then vortexed for *ca.* 10 sec before it was delivered to the vigorously stirred reaction mixture. A Hirsh funnel was used to ensure a continuous delivery of reducing agent. The solution turned dark immediately indicating the formation of nanoparticles. Upon completion of the 3 h reaction, the organic layer was removed and the remaining aqueous layer was dried over rotary evaporation. The resulting crude nanoparticles were suspended in 25 mL of methanol and placed on a frit (F) for additional washing with methanol, ethanol, THF, chloroform, acetonitrile, and acetone. The isolated nanoparticles were re-dissolved in water and placed in dialysis overnight. Pd nanoparticles were isolated after removing water by rotary evaporation and dried under vacuum overnight.

2.4 Functionalization of glass slides

The silanization procedure started with glass microscope slides that were cleaned in a "pirähna" solution (3:1 H_2SO_4:H_2O_2), sonicated in nanopure water for 10 min, rinsed thoroughly with nanopure water and methanol, and placed in a 50 mL methanol solution containing 2 mL of triethyl 3-mercaptopropyl trimethoxysilane and 1 mL of nanopure water for 24 h. *(Caution: Pirähha solution reacts violently with organic materials and should be handled with extreme care.)* The glass slides were rinsed with methanol and ethanol and blown dry with N_2. The prepared glass slides were stored in a dry cabinet for future use.

2.5 Preparation of nanostructured films

For multilayers containing polymer linkers, 10 mg of PAH (M.W. 70,000) was dissolved in 10 mL of nanopure water yielding *ca.* 14 μM solution concentration. To build the nanoparticle multilayers onto glass slides, the MPTS-functionalized glass slides were placed in the aqueous solution containing GS-AuNP (~1.1 ± 0.4 nm in diameter) or MHA-PdNP (~1.2 ± 0.5 nm in diameter) for 24 h (Shon *et al.* 2011). Then, the slides were alternately placed in the aqueous

solution containing PAH and in the respective nanoparticle solution for five min each to build the second layer of the nanoparticle films. The prior step was repeated multiple times to build up a certain number of layers of the nanoparticle multilayer films. To control the structure and composition of the films, the order (e.g., Au-Au-Pd-Pd, Pd-Pd-Au-Au, Pd-Pd-Pd-Pd, or Au-Au-Au-Au) of nanoparticle depositions and the number (4 and 8 nanoparticle layers) of nanoparticle multilayer films were varied.

Nanoparticle multilayer films were then heated in a Barnstead Thermolyne 1300 furnace under air for one hour and characterized by monitoring the changes in the absorbance of nanoparticle films by UV-Vis Spectroscopy (Shon *et al.* 2011). The controlled temperature was set at $600\,℃ \pm 5\,℃$. The heated slides were left to cool in air to room temperature and immediately stored in a dry cabinet.

2.6 Measurements

UV-Vis spectra of nanoparticles and nanostructured films were acquired on Shimazu UV-2450 UV-Vis spectrophotometer equipped with a film (slide) holder. A baseline correction procedure (the spectrum of a standard glass slide was taken as baseline) was executed prior to each measurement session. Infrared spectra were obtained, using a Perkin Elmer Spectrum 100 FT-IR UATR spectrometer, from films on glass microscope slides. The spectra were recorded from 4,000 to 600 cm^{-1}. Transmission electron microscope (TEM) images were obtained with a JEOL 1200 EX II electron microscope operating a 90 keV. Samples were prepared by placing 25 μL of an aqueous Pd nanoparticle solution (~1 mg/mL) on a 200 mesh copper grid with formmvar film. Size distribution analysis of metal nanoparticle core microscope images was executed with Scion Image Beta Release 2^{TM}. Background subtraction was done by Rolling Ball at a set radius of 25. Measurements options were done by Ellipse Major Axis. Topographic height measurements were performed using tapping mode atomic force microscope (AFM) operated in the intermittent contact mode (Nuño *et al.* 2011).

3. Results and discussion

Small and monodispersed Au and Pd nanoparticles were first synthesized for the generation of nanoparticle multilayer films. Glutathione-capped Au_{25} nanoparticles (GS-AuNP; ~1.1 $\pm$ 0.4 nm) were devised by the procedure as reported by Wu 2009. The successful synthesis of these monodispersed particles was confirmed by UV-Vis spectroscopy, which revealed the characteristic bands (Wu and Jin 2009) of this cluster at ~680 nm and ~420 nm (Fig. 1). The result was in a good agreement with TEM data showing small average core size and high monodispersity for GS-AuNP (Fig. 2). The synthesis of small 6-mercaptohexanoic acid-capped Pd nanoparticles (MHA-PdNP; ~1.2 $\pm$ 0.5 nm) was based on our prior studies in which we described thiolate-capped Pd nanoparticle as regioselective chemical catalysts (Gavia *et al.* 2013, Sadeghmoghaddam *et al.* 2012). The core size and monodispersity of MHA-PdNP were evaluated by UV-Vis spectroscopy and TEM (Figs. 1 and 3). The UV-Vis spectrum of MHA-PdNP exhibited an absorbance throughout the entire wavelength range (300 nm to 800 nm) that decays exponentially with increasing wavelength, which is particular to these types of PdNPs (Gavia *et al.* 2013). Moreover, the UV data eliminated the possible presence of any oxidized Pd(II) on the surface or Pd(II)-thiolate species in solution as reasoned by the absence of a broad peak centered at ~450 nm

(Sharma *et al.* 2012). Fig. 3 displays a TEM image of these palladium colloids along with histogram data. Data analysis for over 1,500 species revealed this colloid to possess an average core size of 1.2 ± 0.5 nm. As demonstrated by the histogram, close to 70% of these nanoparticles can be documented as ~1.0 – 1.2 nm in core diameter confirming a relatively good monodispersity of this nanoscale palladium.
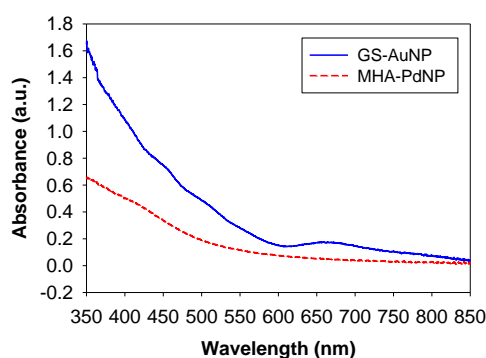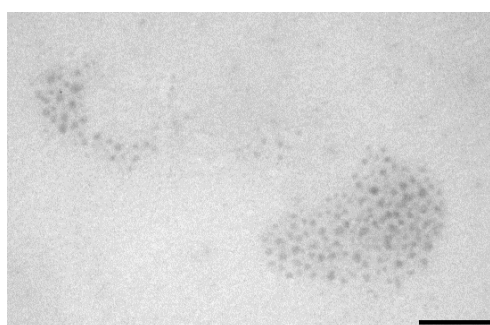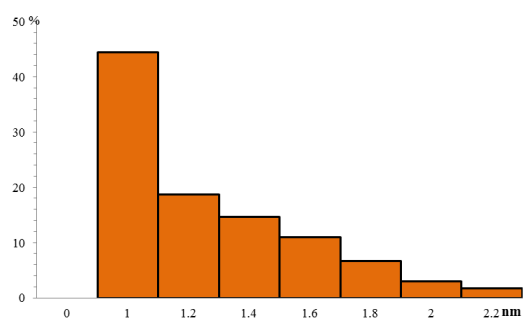

Fig. 1 UV-Vis spectra of glutathione-capped Au_{25} nanoparticles (GS-AuNP) and 6-mercaptohexanoic acid-capped Pd nanoparticles (MHA-PdNP)

| (a) TEM image | (b) Histogram |

Fig. 2 TEM images (size bar: 20 nm) and histograms of glutathione-capped Au_{25} nanoparticles (GS-AuNP)
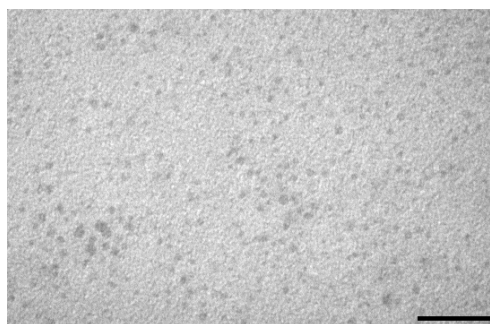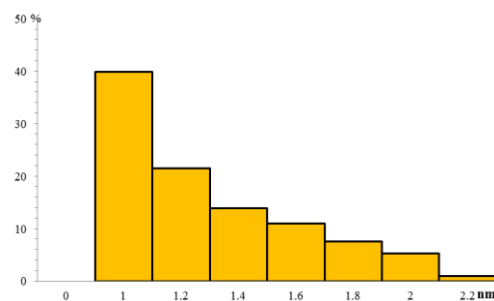
| (a) TEM | (b) Histogram |

Fig. 3 TEM images (size bar: 20 nm) and histograms of 6-mercaptohexanoic acid-capped Pd nanoparticles (MHA-PdNP)
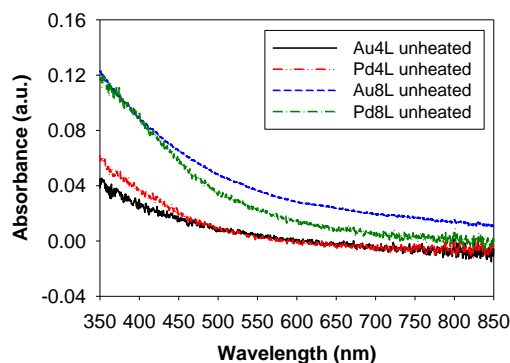
Fig. 4 UV-Vis spectra of Au and Pd nanoparticle multilayer films with 4 and 8 layers before and after heat treatment at 600°C

The layer-by-layer (LbL) films (4 and 8 layers) of small and monodispersed metal nanoparticles (GS-AuNP and MHA-PdNP)-PAH linkers were grown on the surface of reactive glass substrates. To control the structure and composition of the films, the order (e.g., Au-Au-Au-Au (4Au) and Au-Au-Pd-Pd (2Au2Pd)) of nanoparticle depositions were varied. The build-up of nanoparticle multilayers was monitored using UV-Vis spectroscopy. The nanoparticle multilayer films generated from GS-AuNP and MHA-PdNP with 4 layers and 8 layers clearly showed different absorbance intensity without any surface plasmon (SP) bands of gold as shown in Fig. 4. This is because the films are only composed of small metal nanoparticles, which do not exhibit SP bands. The small absorption bands, which are the characteristic peaks of $Au_{25}NP$, shown in Fig. 1 are no longer observed from nanoparticle multilayer films most likely due to the proximity of assembled Au_{25} nanoparticles on glass surfaces and the resulting interactions. The nanoparticle multilayer films generated from MHA-PdNP and the mixture of GS-AuNP and MHA-PdNP also exhibited an absorbance throughout the entire wavelength range that decays exponentially with increasing wavelength without any absorption or SP bands in UV-Vis spectra (Sadeghmoghaddam *et al.* 2011).

We have previously shown that the stable gold nanostructured films are prepared from nanoparticle-PAH multilayer films after heat treatment at 600°C (Shon *et al.* 2011, Vaccarello *et al.* 2012). The particular heating temperature (600°C) was chosen based on our two previous findings. First, heating at a temperature higher than 600°C causes the deterioration (notable shape change) of the glass substrates. Second, the complete removal of surface binders and polymer linkers (PAH) used for building nanoparticle multilayer films requires heating the multilayer films at temperature above 550°C. The FT-IR spectra of silanized glass substrates, nanoparticle multilayer films (Au4L), and heated nanostructed films (4Au) confirmed a complete removal of organic materials after heat treatments at 600°C (Fig. 5), showing only peaks relevant to Si-O bond stretching frequencies for heated 4Au films.

Eight different nanostructured films were prepared by heating nanoparticle multilayer films with different compositions (4Au, 4Pd, 2Au2Pd, 2Pd2Au, 8Au, 8Pd, 4Au4Pd, and 4Pd4Au). Fig. 6 shows that both types of films (4Au and 8Au) heated at 600°C for 1 h display sharp SP bands of gold at around 550-570 nm. This result agreed with our previous work that the nanostructured metallic films were produced through the evaporation of organic molecules from nanoparticle
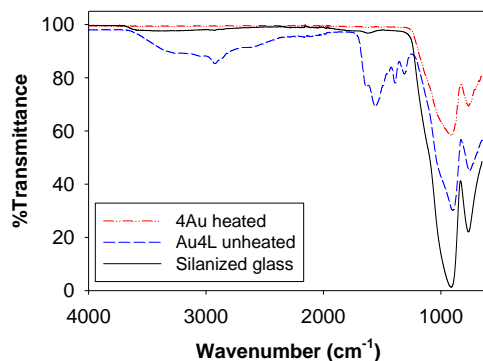
Fig. 5 FT-IR spectrosocpy of glass microscope slide and gold nanoparticle multilayer films (4 layers) before and after heat treatment at 600 °C
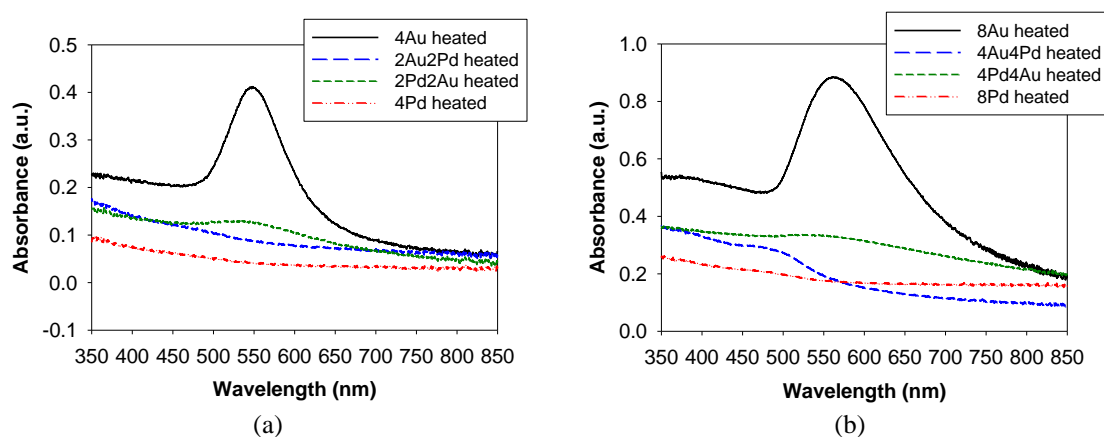

Fig. 6 UV-vis spectra of (a) the heated 4Au, 4Pd, 2Pd2Au, and 2Au2Pd films and (b) the heated 8Au, 8Pd, 4Pd4Au, and 4Au4Pd films

multilayer films, which allow the AuNP to coalescence into larger clusters on the surface of the glass substrates. The less intense SP bands of gold and a faint color of slides for the heated 4Au films are corresponding to the lower density of gold clusters on the glass slides. The SP band of the heated 8Au films was predictively more intense than that of the heated 4Au films indicating the formation of larger clusters with high density. A slightly longer maximum wavelength (λ_{max}) along with some broadening of SP bands was observed for the heated 8Au films indicating somewhat different chemical or physical environment (the shorter distance between the clusters and the increased density of larger aggregated clusters) surrounding the gold clusters compared to that of the heated 4Au films on the glass substrates.

As for the heated 4Pd films, the produced films were visibly different from the heated 4Au films. The nanostructured films generated from the 4Pd films after heating exhibited a faint yellow color which was clearly distinguishable from the faint pink color of the heated 4Au films. UV-Vis spectra of the heated 4Pd films showed an absence of SP bands agreeing with the characteristics of
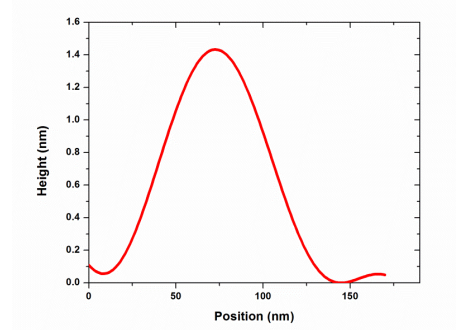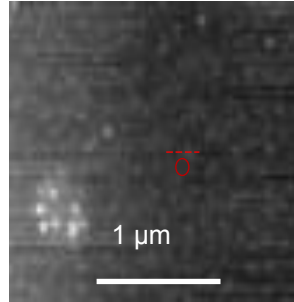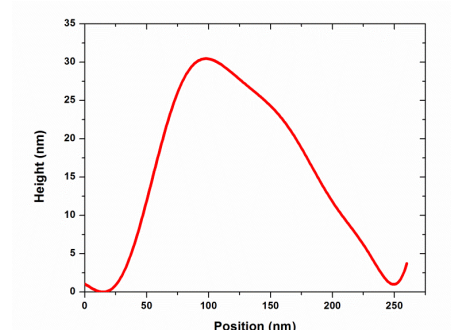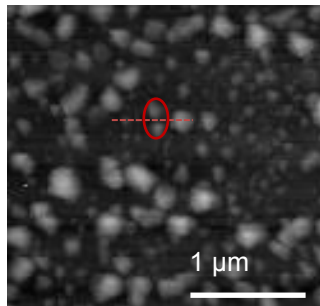
(a) 4Au
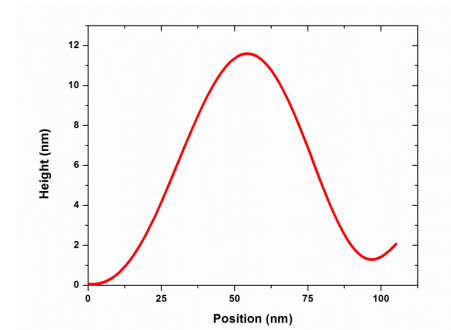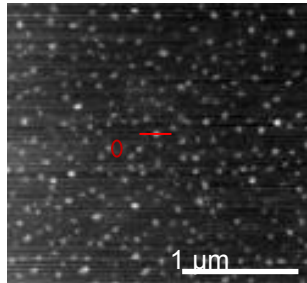
(b) 2Pd2Au
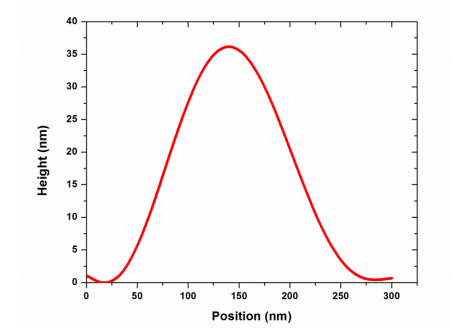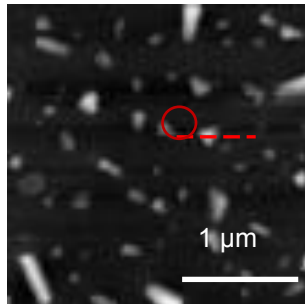
(c) 4Pd

(d) 2Au2Pd

Fig. 7 S-SNOM images and line profiles (a)-(d) of the heated 4Au, 4Pd, 2Pd2Au, and 2Au2Pd films. Metal clusters (particles) appear bright compared to the glass substrate

surface immobilized Pd clusters (Oh *et al.* 2003). Interestingly, the nanostructured films generated from the mixed gold and palladium nanoparticle multilayer films (2Au2Pd and 2Pd2Au) after heating showed distinguishable UV-Vis spectra. UV-Vis spectra of the heated 2Au2Pd films resembled that of the heated 4Pd films exhibiting an absorbance that decays exponentially with increasing wavelength. This clearly indicates that the surface of the heated 2Au2Pd films is mostly composed of Pd atoms. In comparison, UV-Vis spectra of the heated 2Pd2Au clearly showed the presence of the SP bands at ~550 nm, suggesting the presence of clustered Au atoms on the surface of nanostructured films.

As evidenced by Fig. 6, the absorbance of the heated films seems to increase with the increased number of layers on the glass slides for each film. The heated 8Au and 4Pd4Au films exhibited the SP bands of gold at ~570 nm. The films with PdNP on the outer layers (the heated Pd and 4Au4Pd films) clearly showed the characteristics of Pd films. A distinct peak at ~500 nm observed for the heated 4Pd4Au films indicated the presence of some small clustered Au atoms on the surface of nanostructured films.

In Fig. 7, we show topographic images on the heat treated nanoparticle multilayer films (4Au, 4Pd, 2Au2Pd, and 2Pd2Au) are presented. The images confirmed that the heat treatments of nanoparticle multilayer films result in the nucleation of nanoparticles and the formation of metallic cluster structures. The images also indicated that the shape of the clusters generated from the 4Au and 2Pd2Au films are highly uniform and spherical. By taking line profiles, we measured the sizes of the nanostructured films to be about 1.5 nm and 11 nm, respectively. The average sizes of these clusters are quite smaller than the heated films generated from the other two multilayer films (4Pd and 2Au2Pd; 36 and 31 nm). The images clearly showed the high populations of rod, rectangle, and triangle-shaped clusters (particles) from the heated 4Pd films. The high polydispersity in the size and shape of clusters is observed from the heated 2Au2Pd films. These results demonstrated the topological responses of the monometallic and bimetallic nanoisland films are greatly affected by the deposition method of nanoparticle multilayer films and the type of nanoparticles incorporated.

4. Conclusions

The preparation of Au, Pd, and Au-Pd nanostructured films are successfully achieved through the method of building and heating nanoparticle multilayer films. The SP bands of gold are observed only when the nanoparticle multilayer deposition is ended with the assembly of gold nanoparticle layers. The results confirm that different composition and layering sequence of nanoparticle multilayer films clearly affects the coalescence behavior of nanoparticles during heat treatments. Further studies are necessary for better understanding the evolution mechanism of bimetallic nanostructured films during heat treatment.

Acknowledgments

References

Gavia, D.J., Maung, M.S. and Shon, Y.S. (2013), "Water-soluble Pd nanoparticles synthesized from ω-carboxyl-*S*-alkanethiosulfate ligand precursors as unimolecular micelle catalysts", *ACS Appl. Mater. Interf.*, **5**(23), 12432-12440.

Hrbek, J., Hoffmann, F.M., Park, J.B., Liu, P., Stacchiola, D., Hoo, Y.S., Ma, S., Nambu, A., Rodriguez, J.A. and White, M.G. (2008), "Adsorbate-driven morphological changes of a gold surface at low temperature", *J. Am. Chem. Soc.*, **130**(51), 17272-17273.

Jones, A.C., Berweger, S., Wei, J., Cobden, D. and Raschke, M.B. (2010), "Nano-optical investigations of the metal-insulator phase behavior of individual VO2 microcrystals", *Nano Lett.*, **10**(5), 1574-1581.

Karakouz, T., Holder, D., Goomanovsky, M., Vaskevich, A. and Rubinstein, I. (2009), "Morphology and refractive index sensitivity of gold island films", *Chem. Mater.*, **21**(24), 5875-5885.

Lee, S.J., An, H.H., Han, W.B., Kim, H.S. and Yoon, C.S. (2012), "Effect of temperature and humidity on coarsening behavior of Au nanoparticles embedded in liquid crystalline lipid membrane", *Langmuir*, **28**(30), 10980-10987.

Lohse, S.E., Dahl, J.A. and Hutchison, J.E. (2010), "Direct synthesis of large water-soluble functionalized gold nanoparticles using Bunte salts as ligand precursors", *Langmuir*, **26**(10), 7504-7511.

Nuño, Z., Hessler, B., Ochoa, J., Shon, Y.S., Bonney, C. and Abate, Y. (2011), "Nanoscale subsurface- and material-specific identification of single nanoparticles", *Optics Express*, **19**(21), 20865-20875.

Oh, S.K., Kim, Y.G., Ye, H. and Crooks, R.M. (2003), "Synthesis, characterization, and surface immobilization of metal nanoparticles encapsulated within bifunctionalized dendrimers", *Langmuir,* **19**(24), 10420-10425.

Sadeghmoghaddam, E., Gu, H. and Shon, Y.S. (2012), "Pd nanoparticle-catalyzed isomerization vs. hydrogenation of allyl alcohol: solvent-dependent regioselectivity", *ACS Catal.*, **2**(9), 1838-1845.

Sadeghmoghaddam, E., Lam, C., Choi, D. and Shon, Y.S. (2011), "Synthesis and catalytic property of alkanethiolate-protected Pd nanoparticles generated from sodium S-dodecylthiosulfate", *J. Mater. Chem.* **21**(2), 307-312.

Scarpettini, A.F. and Bragas, A.V. (2010), "Coverage and aggregation of gold nanoparticles on silanized glasses", *Langmuir*, **26**(20), 15948-15953.

Sharma, S., Kim, B. and Lee, D. (2012), "Water-soluble Pd nanoparticles capped with glutathione: synthesis, characterization, and magnetic properties", *Langmuir*, **28**(45), 15958-15965.

Shon, Y.S., Aquino, M., Pham, T.V., Rave, D., Ramirez, M., Lin, K., Vaccarello, P., Lopez, G., Gredig, T. and Kwon, C. (2011), "Stability and morphology of gold nanoisland arrays generated from layer-by-layer assembled nanoparticle multilayer films: effects of heating temperature and particle size", *J. Phys. Chem. C*, **115**(21), 10597-10605.

Srivastava, S. and Kotov, N.A. (2008), "Composite layer-by-layer (LBL) assembly with inorganic nanoparticles and nanowires", *Acc. Chem. Res.*, **41**(12), 1831-1841.

Stewart, M.E., Anderton, C.R., Thompson, L.B., Maria, J., Gray, S.K., Rogers, J.A. and Nuzzo, R.G. (2008), "Nanostructured plasmonic sensors", *Chem. Rev.*, **108**(2), 494-521.

Sugden, M.W., Richardson, T.H. and Leggett, G. (2010), "Sub-10 Ω resistance gold films prepared by removal of ligands from thiol-stabilized 6 nm gold nanoparticles", *Langmuir*, **26**(6), 4331-4338.

Sun, H., Yu, M., Sun, X., Wang, G. and Lian, J. (2013), "Effective temperature sensing by irreversible morphology evolution of ultrathin gold island films", *J. Phys. Chem. C*, **117**(7), 3366-3373.

Szunerlts, S., Das, M.R. and Boukherroub, R. (2008), "Short- and long-range sensing on gold nanostructures, deposited on glass, coated with silicon oxide films of different thicknesses", *J. Phys. Chem. C*, **112**(22), 8239-8243.

Vaccarello, P., Tran, L., Meinen, J., Kwon, C., Abate, Y. and Shon, Y.S. (2012), "Characterization of localized surface plasmon resonance transducers produced from Au$_{25}$ nanoparticle multilayers", *Colloid. Surf., A*, **402**, 146-151.

Wu, Z., Suhan, J. and Jin, R. (2009), "One-pot synthesis of atomically monodisperse, thiol-functionalized

Au$_{25}$ nanoclusters", *J. Mater. Chem.*, **19**(5), 622-626.

Wu, Z. and Jin, R. (2009), "Stability of the two Au-S binding modes in Au$_{25}$(SG)$_{18}$ nanoclusters probed by NMR and optical spectroscopy", *ACS Nano*, **3**(7), 2036-2042.

Zamborini, F.P., Bao, L. and Dasari, R. (2012), "Nanoparticles in measurement science", *Anal. Chem.*, **84**(2), 541-576.

CC